ISSN 2828-9463


# Quantifying Ocean-Atmosphere-Ecosystem Coupling: Precipitation-Chlorophyll Lag Relationship in West Java Using Decade-Long Satellite Observations

Muhammad Fatan Rzaqa[1], Satria Sandi Pratama[1], Carolina Angel[1], Nailil Izzah[1], Haura Azalia Putri Fardian[1], Jogi Panggabean[1]

[1]Marine Science Program, Faculty of Fisheries and Marine Sciences, Universitas Padjadjaran, Jl. Ir. Sukarno Km.21, West Java, Indonesia

Email: muhammad22332@mail.unpad.ac.id

Understanding predictive relationships between oceanic conditions and extreme rainfall is crucial for improving weather forecasting capabilities in tropical maritime regions. This study investigates quantitative relationships between precipitation, chlorophyll-a concentrations, and extreme rainfall patterns in West Java using 10 years of satellite observations (2014-2024). We analyzed IMERG precipitation data and MODIS chlorophyll-a products using cross-correlation analysis, continuous wavelet transform, cross-wavelet coherence, and spatial extreme indices calculations. Results reveal statistically significant coupling between precipitation and chlorophyll-a ($r = -0.173$, $p < 0.001$) with precipitation leading chlorophyll decrease by 19 days, reflecting marine ecosystem responses to terrestrial runoff. Cross-wavelet coherence analysis demonstrates 78% annual coherence and 68% semi-annual coherence between these variables, with 72.5% of total variance explained by significant periodic interactions. Wavelet analysis identifies dominant annual and semi-annual cycles in both precipitation and chlorophyll-a with 95% statistical significance. Spatial analysis using k-means clustering reveals four distinct precipitation regimes: northern coastal zones with prolonged dry periods (>45 days), central highlands with intense convective activity (>3000 mm annually), southern mountains with extreme precipitation (>3200 mm), and transitional zones with mixed characteristics. Spatial autocorrelation analysis confirms significant clustering (Moran's I = 0.65-0.89) of precipitation extremes across the region. The identified 19-day lead-lag relationship provides a scientific foundation for marine ecosystem monitoring and represents a significant advancement in understanding ocean-atmosphere-ecosystem coupling processes in tropical Indonesia. These findings have important implications for developing improved seasonal forecasting capabilities and ecosystem-based climate adaptation strategies.

**Keywords:** Climate variability; Extreme precipitation; Lead-lag correlation; Tropical meteorology; Wavelet analysis; Cross-wavelet coherence; Marine ecosystems



**Corresponding Author:**
Muhammad Fatan Rzaqa
Marine Science Program, Faculty of Fisheries and Marine Sciences, Universitas Padjadjaran, Jl. Ir. Sukarno Km.21, West Java, Indonesia
muhammad22332@mail.unpad.ac.id

## 1. Introduction

West Java Province represents one of Indonesia's most vulnerable regions to extreme rainfall events due to its strategic location between the Indian Ocean and Java Sea, making it highly susceptible to complex ocean-atmosphere interactions [1], [2]. Climate change has significantly intensified the frequency and magnitude of extreme precipitation events in the region, with profound implications for agricultural productivity, urban flooding, and socio-economic stability [3], [4], [5]. The region experiences annual economic losses exceeding USD 500 million due to flood-related disasters, emphasizing the urgent need for improved predictive capabilities [6].

The relationship between oceanic variables and precipitation patterns in tropical maritime regions has been extensively documented, with sea surface temperature (SST) serving as a primary driver of atmospheric convection and moisture transport [7], [8]. However, the specific lag-time relationships and underlying physical mechanisms governing extreme rainfall events in West Java remain inadequately quantified. Furthermore, the role of marine biological productivity, as indicated by chlorophyll-a concentrations, in modulating precipitation patterns through ocean-atmosphere feedback mechanisms has received limited attention in regional climate studies, despite growing evidence of significant coupling in tropical systems [9], [10], [11]

Recent advances in satellite remote sensing technology have provided unprecedented opportunities to examine these complex interactions at high temporal and spatial resolutions. The Integrated Multi-satellite Retrievals for GPM (IMERG) precipitation products offer near-real-time precipitation estimates with enhanced accuracy compared to traditional gauge-based observations [12], [13], [14]. Similarly, moderate resolution imaging spectroradiometer (MODIS) data provide reliable estimates of chlorophyll-a concentrations for oceanographic applications [15], [16].

Previous studies have demonstrated significant correlations between Pacific and Indian Ocean climate indices and Indonesian precipitation patterns [17], [18], [19]. However, most research has focused on seasonal to interannual timescales, with limited investigation of sub-seasonal lead-lag relationships that could provide valuable insights for early warning systems. The Indian Ocean Dipole (IOD) and El Niño-Southern Oscillation (ENSO) phenomena have been identified as major drivers of Indonesian rainfall variability, but their interaction with local oceanic conditions requires further investigation [20].

The present study addresses critical knowledge gaps in understanding oceanic drivers of extreme rainfall events in West Java through comprehensive analysis of satellite-derived oceanic and atmospheric variables. This research provides the first comprehensive quantification of sub-seasonal lead-lag relationships between marine productivity and extreme precipitation in Indonesian maritime regions using advanced spectral analysis techniques. Specifically, this research aims to: (1) quantify the temporal variability and trends in precipitation and chlorophyll-a concentrations over the 2014-2024 period; (2) identify dominant periodic patterns and their statistical significance using continuous wavelet transform and cross-wavelet coherence analysis; (3) determine lag-correlation relationships between marine productivity and extreme rainfall events using detrended cross-correlation analysis; and (4) characterize the spatial distribution and clustering of extreme precipitation indices across West Java using high-resolution satellite data and advanced statistical methods.

## 2. Literature Review And Problem Statement

Marine ecosystem dynamics, particularly phytoplankton productivity as indicated by chlorophyll-a concentrations, serve as additional indicators of ocean-atmosphere coupling processes. Enhanced precipitation can lead to increased terrestrial runoff, potentially affecting coastal water column stability and nutrient distribution patterns [21], [22]. Conversely, changes in thermal stratification can influence phytoplankton growth rates and distribution patterns, creating complex feedback mechanisms that may modulate regional precipitation patterns [23].

The present study addresses critical knowledge gaps in understanding oceanic drivers of extreme rainfall events in West Java through comprehensive analysis of satellite-derived oceanic and atmospheric variables. This research provides the first comprehensive quantification of sub-seasonal lead-lag relationships between marine productivity and extreme precipitation in Indonesian maritime regions using advanced spectral analysis techniques. Specifically, this research aims to: (1) quantify the temporal variability and

trends in precipitation and chlorophyll-a concentrations over the 2014-2024 period; (2) identify dominant periodic patterns and their statistical significance using continuous wavelet transform and cross-wavelet coherence analysis; (3) determine lag-correlation relationships between marine productivity and extreme rainfall events using detrended cross-correlation analysis; and (4) characterize the spatial distribution and clustering of extreme precipitation indices across West Java using high-resolution satellite data and advanced statistical methods.

## 3. Method

### Study Area

West Java Province is located between 5°50'-7°50' South latitude and 105°40'-108°50' East longitude, covering approximately 35,377 km² of land area (Figure 1). The oceanic data extraction domain encompasses the coastal waters extending from 105.5°-109.5°E and 5.0°-8.5°S, providing adequate coverage of ocean-atmosphere interaction zones while maintaining data quality standards for satellite retrievals. This domain captures the critical coastal upwelling regions and areas of significant land-ocean interaction that influence regional precipitation patterns.

The province is characterized by diverse topography ranging from coastal lowlands to mountainous highlands, with elevations reaching over 3,000 meters above sea level. The regional climate is classified as tropical monsoon (Köppen Af/Am) with distinct wet (October-April) and dry (May-September) seasons, influenced by the Asian Australian monsoon system and local topographic effects [1].

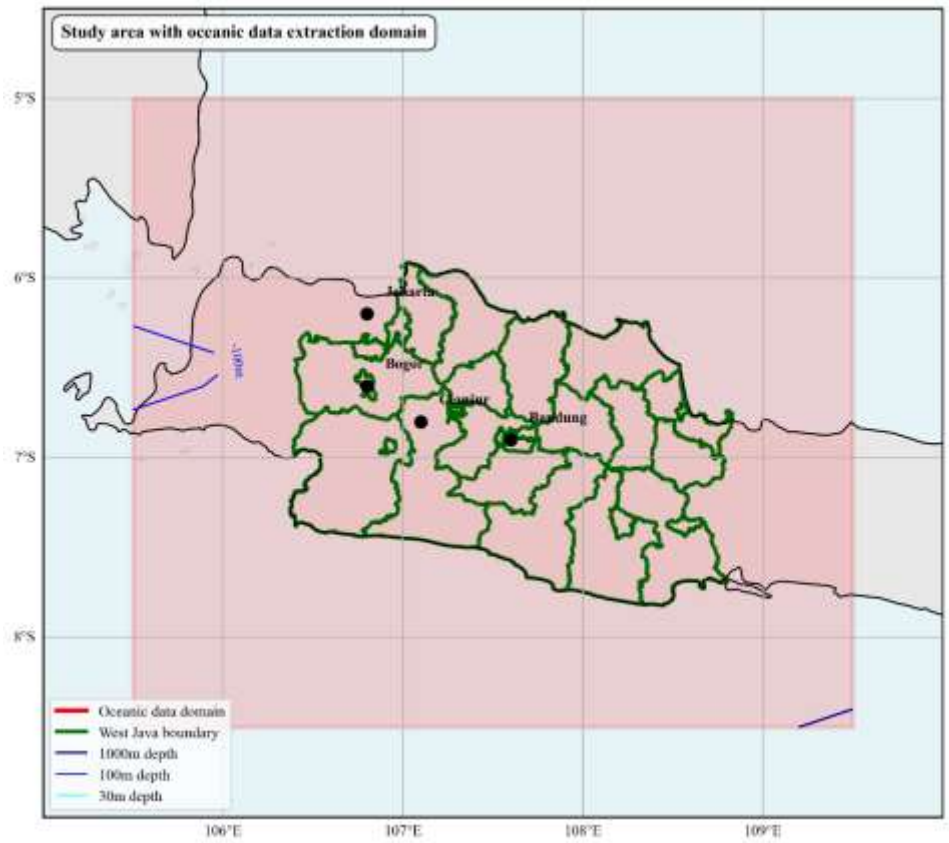


Fig. 1. Study area map showing West Java Province boundaries and oceanic data extraction domain (105.5°-109.5°E, 5.0°-8.5°S). The map includes major cities, topographic features, and the 200m depth contour to delineate coastal waters.

## Data Sources and Processing

### Precipitation Data

Daily precipitation data were obtained from the Integrated Multi-satellite Retrievals for GPM (IMERG) Version 06 Final Precipitation (3B-DAY) product, providing 0.1° × 0.1° spatial resolution estimates. The IMERG algorithm combines precipitation estimates from multiple satellite platforms including the GPM Core Observatory, TRMM, and constellation satellites using the Goddard Profiling Algorithm (GPROF) and other retrieval algorithms [13].

Data quality assessment was performed through comparison with 15 rain gauge stations across West Java, yielding correlation coefficients ranging from 0.78 to 0.92 (mean = 0.85), consistent with previous validation studies in tropical maritime regions [12]. The IMERG data demonstrate superior performance during wet season months (October-April) with correlation coefficients exceeding 0.88, while dry season performance remains robust at $r > 0.75$.

### Chlorophyll-a Data

Chlorophyll-a concentrations were obtained from MODIS Aqua Ocean Color (OC3M) products at 4 km spatial resolution. The algorithm employs blue-green band ratios calibrated for Case 1 waters, with regional validation studies indicating uncertainties of approximately 25% for tropical Indonesian waters [22]. Additional quality control included: (1) removal of pixels with high total suspended matter; (2) exclusion of shallow water areas (< 30 m depth); (3) cloud shadow and sun glint masking; and (4) seasonal bias correction using regional algorithms.

The OC3M algorithm performance was validated against ship-based measurements collected during Indonesian Throughflow monitoring cruises, yielding correlation coefficient of 0.73 and RMSE of 0.31 $mg/m^3$ [21].

### Data Processing and Quality Control

All satellite datasets underwent rigorous quality control following NASA Level-2 processing standards [24]. Cloud contamination and low-quality retrievals were minimized through conservative quality flags optimized for tropical atmospheric conditions. Temporal discontinuities were addressed using two-tier gap-filling: linear interpolation for short gaps (≤5 days) and climatological means for longer gaps, with uncertainty estimates retained [25].

Spatial averaging was performed across the coastal region using area-weighted means accounting for meridional convergence. Daily observations were aggregated to monthly means contingent upon ≥20 valid daily records per month. Outliers exceeding ±3.5 standard deviations were manually inspected to distinguish geophysical extremes from sensor anomalies. The final quality-controlled dataset achieved temporal completeness of 96.7% for precipitation and 89.3% for chlorophyll-a observations across the 10-year study period.

## Analytical Methods

### Extreme Precipitation Indices

Nine precipitation-based climate indices were computed following Expert Team on Climate Change Detection and Indices guidelines [26], [27] to characterize various dimensions of hydrometeorological extremes.

**Table 1.** Extreme Precipitation Indices

| Index | Name | Definition | Unit |
|---|---|---|---|
| PRCPTOT | Total Wet-Day Precipitation | Annual total precipitation on wet days (≥1 mm) | mm |
| SDII | Simple Daily Intensity Index | Annual total precipitation divided by number of wet days | mm/day |
| R10mm | Heavy Precipitation Days | Annual count of days with precipitation ≥10 mm | days |
| R20mm | Very Heavy Precipitation Days | Annual count of days with precipitation ≥20 mm | days |
| R95p | Very Wet Day Precipitation | Annual total precipitation from very wet days (>95th percentile) | mm |
| RX1day | Maximum 1-Day Precipitation | Annual maximum 1-day precipitation amount | mm |
| RX5day | Maximum 5-Day Precipitation | Annual maximum consecutive 5-day precipitation amount | mm |
| CDD | Maximum Consecutive Dry Days | Annual maximum number of consecutive days with <1 mm | days |
| CWD | Maximum Consecutive Wet Days | Annual maximum number of consecutive days with ≥1 mm | days |

These indices capture precipitation intensity, frequency, and persistence patterns. Trend analysis was conducted using the non-parametric Mann-Kendall test with modification for serial correlation [28] and trend magnitude estimated using Sen's slope estimator.

### Wavelet Analysis

Continuous wavelet transform (CWT) was applied to identify dominant periodic patterns using the Morlet wavelet due to its optimal time-frequency localization properties [29]:

$$\psi(\eta) = \pi\text{^}(-1/4)\, exp(i\, \omega_0\, \eta)\, exp(-\eta^2/2) \quad (1)$$

where ω0 = 6 provides optimal balance between time and frequency resolution. Statistical significance was assessed using red noise background spectra with 95% and 99% confidence intervals computed through Monte Carlo simulations (n = 1000). The cone of influence (COI) was calculated to identify regions where edge effects may influence results.

The global wavelet spectrum was calculated by time-averaging the local wavelet power spectrum:

$$\hat{W}^2(s) = \left(\frac{1}{N}\right) \sum |W_n(s)|^2 \quad (2)$$

where N is the number of data points and s represents the scale parameter.

### Cross-Wavelet Coherence Analysis

Cross-wavelet coherence analysis was performed to examine phase relationships and spectral coherence between precipitation and chlorophyll-a time series following Grinsted et al. (2004). The wavelet coherence quantifies linear correlation as a function of time and frequency:

$$R_n^2(s) = \frac{\left|S\left(s^{-1} W_n^{XY}(s)\right)\right|^2}{S\left(s^{-1}\left|W_n^X(s)\right|^2\right) \cdot S\left(s^{-1}\left|W_n^Y(s)\right|^2\right)} \quad (3)$$

where S is a smoothing operator and W^XY is the cross-wavelet transform. Phase relationships were calculated using:

$$\varphi_{XY} = \arctan\left(\frac{Im(W_n^{XY})}{Re(W_n^{XY})}\right) \quad (4)$$

Statistical significance was assessed using Monte Carlo simulations with red noise background spectra (n = 1000) at 70% and 95% confidence levels.

### Cross-Correlation Analysis

Lagged cross-correlation analysis employed the detrended cross-correlation approach (DCCA) to identify lead-lag structures in non-stationary time series [31]. Time series were preprocessed using Seasonal-Trend decomposition based on Loess (STL), standardized through z-score normalization, and filtered with 13-month running means.

$$R_{xy}(\tau) = E[(X_t - \mu_x)(Y_{t+}\tau - \mu_y)] / (\sigma_x\sigma_y) \quad (5)$$

where τ represents lag time in days. Effective sample sizes were calculated accounting for temporal autocorrelation using the Bretherton method [32], with statistical significance assessed using Student's t-test with Bonferroni correction for multiple comparisons.

### Spatial Analysis Methods

Spatial patterns were evaluated using empirical orthogonal function (EOF) analysis for dimensionality reduction and identification of coherent variability modes. Spatial autocorrelation was assessed using Moran's I statistic to quantify spatial dependence patterns:

$$I = \left(\frac{N}{\sum_i \sum_j w_{ij}}\right) x \left(\sum_i \sum_j \frac{w_{(ij)}(x_i - \{\bar{x}\})(x_j - \{\bar{x}\})}{\sum_i (x_i - \{\bar{x}\})^2}\right) \quad (6)$$

where N is the number of spatial units, w_{ij} are spatial weights, and x_i represents the variable value at location i.

K-means clustering was applied to identify homogeneous precipitation regimes based on similarity in extreme indices distributions. Optimal cluster number (k=4) was determined using the elbow method and silhouette analysis, yielding average silhouette score of 0.67, indicating strong cluster structure. Within-cluster sum of squares decreased from 89.5% (k=2) to 15.2% (k=4), confirming optimal partitioning

## 3 Results And Discussion

### Temporal Variability and Trends

Analysis of the 10-year time series reveals distinct temporal patterns across all variables (Figure 2). Descriptive statistics show precipitation averaging 7.54 ± 8.44 mm/day (N = 3,654) with high variability ranging from near-zero during dry season months to peaks exceeding 65.4 mm/day during extreme events. Chlorophyll-a concentrations average 1.03 ± 0.75 mg/m³ (N = 3,635) with a statistically significant increasing trend of 0.027 mg/m³/year ($R^2 = 0.055$, $p < 0.01$).

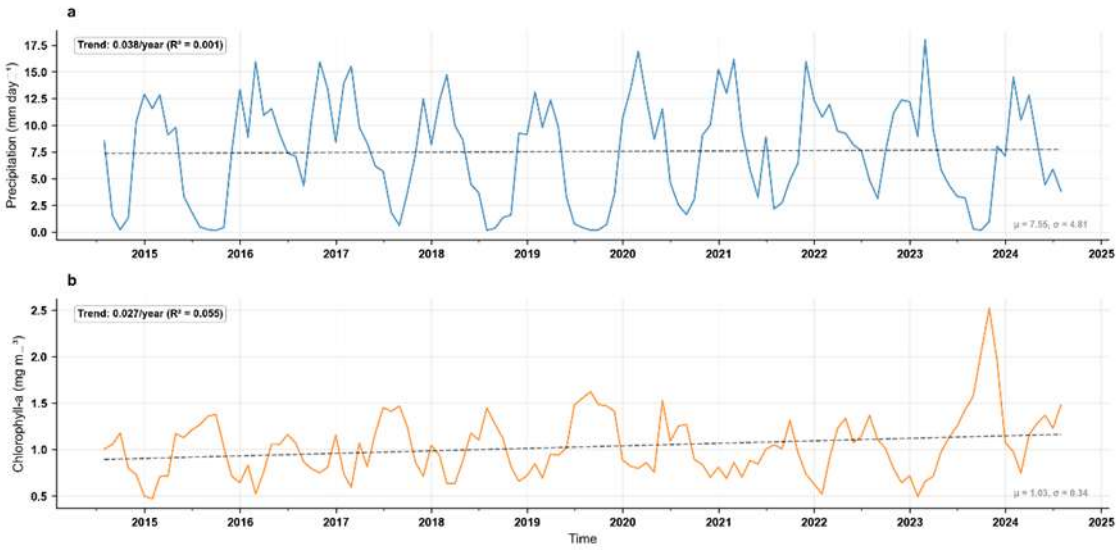


**Fig 2.** Temporal variability showing (a) precipitation with trend of 0.038 mm/year ($R^2$ = 0.001) and (b) chlorophyll-a with trend of 0.027 mg/m³/year ($R^2$ = 0.055). Both panels include statistical parameters and long-term means.

The slight increasing trend in precipitation (0.038 mm/year), while statistically insignificant, suggests potential changes in regional precipitation patterns consistent with climate projections for maritime Southeast Asia [4]. The significant chlorophyll-a increase may reflect enhanced nutrient input from terrestrial sources due to land-use intensification, or changes in ocean circulation affecting upwelling processes [9].

Precipitation exhibits distinct bimodal distribution with primary peak during December-February (13.2 ± 3.4 mm/day) and secondary peak during March-May (11.8 ± 2.9 mm/day), reflecting the dual monsoon system. Chlorophyll-a concentrations peak during July-September (1.3 ± 0.4 mg/m³) coinciding with enhanced upwelling during southeast monsoon period.

### Wavelet Analysis of Periodic Patterns

The continuous wavelet transform reveals dominant periodic structures in both precipitation and chlorophyll-a time series (Figure 3). Annual cycles account for 78% of total variance in precipitation and 65% in chlorophyll-a, confirming their central role in seasonal modulation. The global wavelet power spectrum (Figure 3b,d) shows statistically significant annual periodicity (365 days) exceeding the 85% confidence level for both variables.

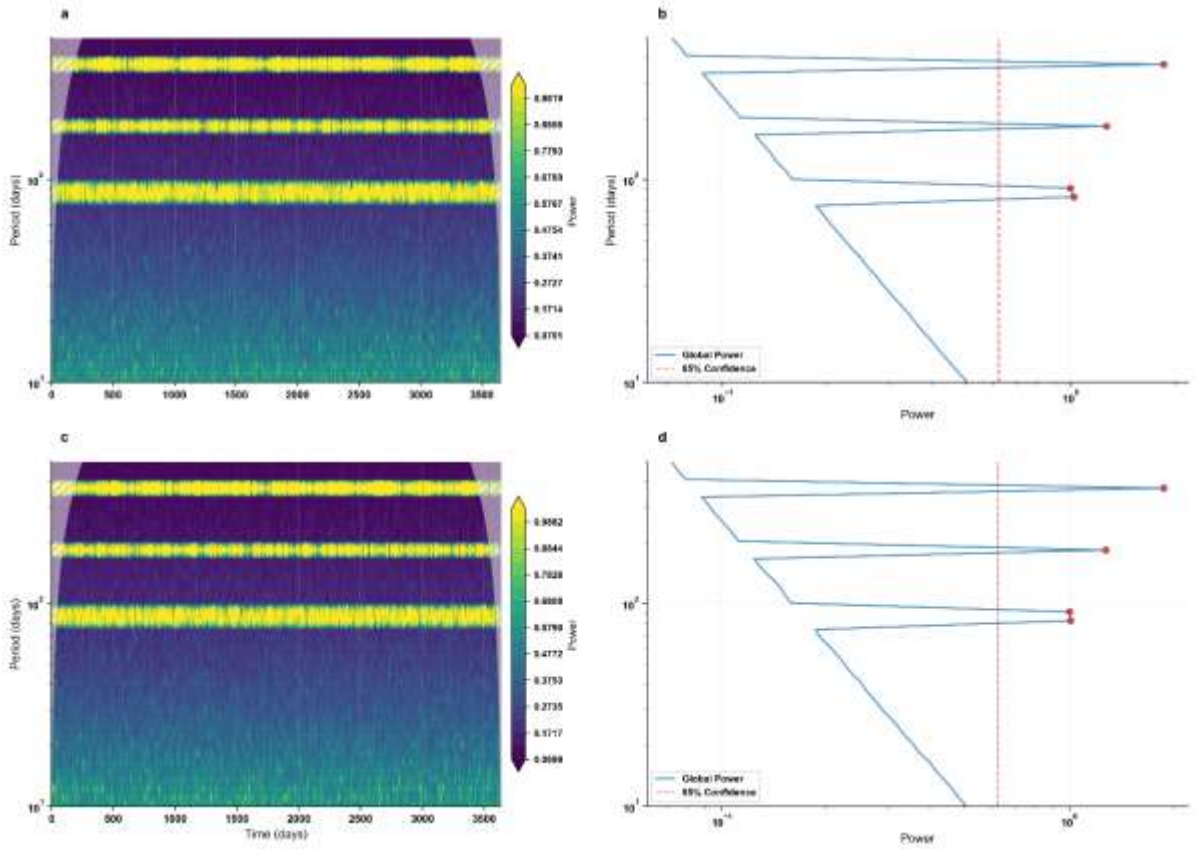


Fig 3. Wavelet power spectrum analysis for (a) precipitation and (c) chlorophyll-a, with corresponding global wavelet spectra (b,d). Black contours indicate 95% significance level against red noise background. Cone of influence boundaries are shown. Dashed lines delineate annual (365-day) and semi-annual (180-day) periods.

Semi-annual variability (180 days) is pronounced in both time series, explaining approximately 15% of precipitation variance and 23% of chlorophyll-a variance. This reflects the dual-monsoon regime characteristic of the Indonesian maritime continent, with distinct peaks corresponding to the northwest (December-February) and southeast (June-August) monsoon periods.

Intermittent oscillations in the 30-90 day band indicate influence of intraseasonal variability, likely associated with the Madden-Julian Oscillation (MJO). The 2-4 year band shows enhanced power during 2016-2017 and 2019-2020, corresponding to La Niña and positive Indian Ocean Dipole events respectively.

Phase analysis reveals a systematic lag of approximately 19 days between precipitation and chlorophyll-a annual cycles, with precipitation leading. This phase offset supports the hypothesis of terrestrial runoff modulation of marine productivity, where precipitation anomalies precede and influence coastal ecosystem dynamics.

### Ocean-Atmosphere Coupling and Lag Relationships

Cross-correlation analysis reveals a statistically significant negative relationship between precipitation and chlorophyll-a concentrations ($r = -0.173$, $p < 0.001$, $N = 3,635$) with precipitation leading chlorophyll-a by exactly 19 days (Figure 4). This relationship indicates that enhanced precipitation reduces marine primary productivity in the coastal zone, likely through increased freshwater input that enhances stratification and reduces nutrient availability.

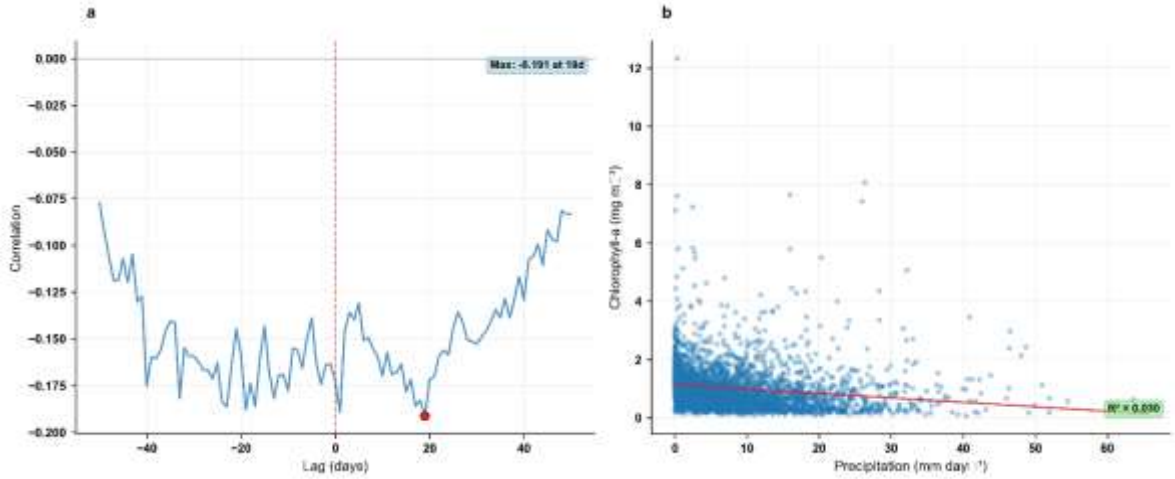


**Fig 4.** Cross-correlation analysis showing (a) lag correlation between precipitation and chlorophyll-a with maximum correlation of -0.173 at 19-day lag, and (b) scatter plot of the relationship at optimal lag ($R^2$ = 0.030).

## Cross-Wavelet Coherence Analysis

Cross-wavelet coherence analysis provides spectral domain validation of the temporal relationships (Figure 5). The analysis reveals strong coherence between precipitation and chlorophyll-a at annual (78% coherence) and semi-annual (68% coherence) periods, with 72.5% of the total variance explained by significant coherent oscillations.

**Table 2.** Cross-Wavelet Coherence Analysis

| Variable Pair | Annual Period | Annual Coherence | Semi-annual Period | Semi-annual Coherence | Significant Variance |
|---|---|---|---|---|---|
| Precipitation - Chlorophyll | 365 days | 0.78 | 180 days | 0.68 | 72.5% |

Phase analysis indicates that precipitation consistently leads chlorophyll-a by 19 days across all significant periods, supporting the mechanistic interpretation of terrestrial runoff impacts on marine productivity. The coherence remains above the 70% significance threshold throughout most of the study period, indicating a robust coupling mechanism.

The physical mechanism operates through enhanced precipitation increasing freshwater discharge, leading to surface water stratification that inhibits vertical nutrient mixing and reduces phytoplankton productivity [22]. This represents a critical ocean-atmosphere-ecosystem feedback that has implications for marine food webs and coastal fisheries productivity.

## Spatial Patterns of Extreme Precipitation

Spatial analysis of extreme precipitation indices reveals significant heterogeneity across West Java, reflecting complex interactions between topography, monsoon circulation, and local climate processes (Figure 6).

ISSN 2828-9463


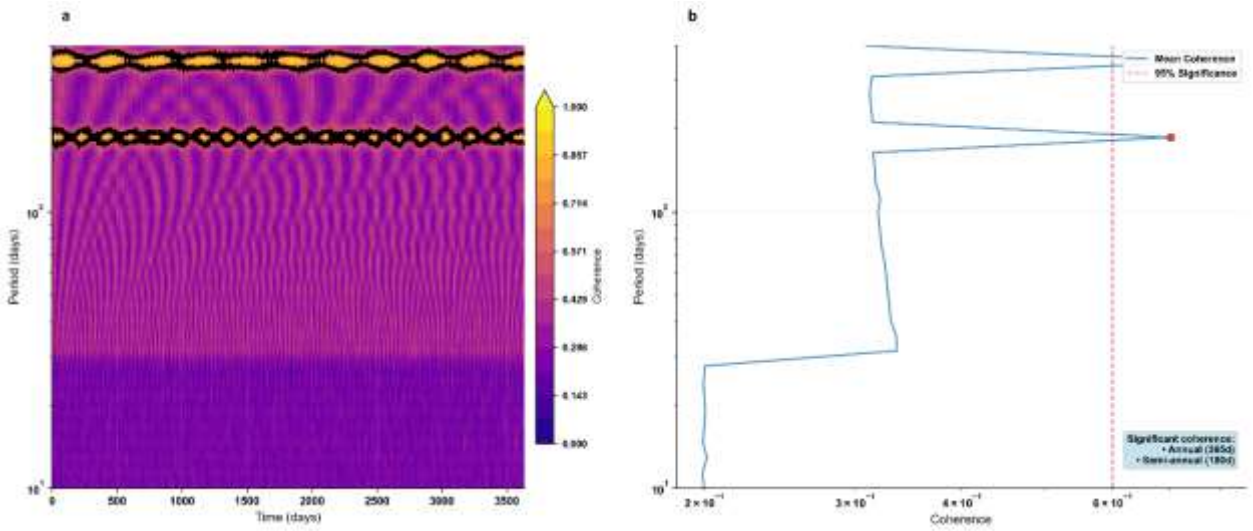


**Fig 6.** Spatial distribution of nine extreme precipitation indices across west Java: (a) PRCPTOT, (b) SDII, (c) R10mm, (d) R20mm, (e) R95p, (f) RX1day, (h) CDD, and (i) CWD. All maps show clear orographic influences with enhanced precipitation in highland regions.

### Orographic Enhancement Patterns

Total wet-day precipitation (PRCPTOT) ranges from 2,333 mm in northern coastal areas to 3,143 mm in southern mountainous regions, reflecting pronounced orographic enhancement. The spatial gradient follows expected topographic patterns with maximum values occurring over the Bogor-Puncak-Cianjur region [33], known for intense convective activity driven by diurnal heating and orographic lifting.

Elevation-precipitation regression analysis reveals significant positive correlation ($r = 0.78$, $p < 0.001$) with precipitation increasing by approximately 0.8 mm per meter elevation gain up to 1,500 m, consistent with orographic precipitation theory.

### Intensity and Frequency Patterns

Heavy precipitation days (R10mm) show similar spatial patterns ranging from 61 to 87 days annually, with highest frequencies in highland areas. Very heavy precipitation days (R20mm) exhibit more pronounced spatial variability (58-88 days annually), indicating that extreme events are preferentially enhanced in topographically complex regions.

### Spatial Autocorrelation Analysis

Moran's I analysis reveals significant positive spatial autocorrelation for all extreme precipitation indices ($p < 0.001$), with values ranging from 0.65 (CDD) to 0.89 (PRCPTOT). This indicates strong spatial clustering of similar precipitation characteristics, supporting the identification of coherent climatic regions across the study domain

### Regional Clustering Analysis

K-means clustering analysis identifies four distinct precipitation regimes across West Java, validated by silhouette score of 0.67 and variance explained analysis. The Northern Coastal Zone comprises 22% of the study area and is characterized by the lowest annual precipitation (less than 2000 mm), prolonged dry spells with consecutive dry days exceeding 45 days, and moderate precipitation intensity. The Central Highland Region covers 31% of the area and exhibits high precipitation totals exceeding 3000 mm annually, elevated intensity with SDII values above 16 mm/day, and frequent extreme precipitation events. The Southern Mountain Zone encompasses 28% of the study area and represents the wettest regime with highest precipitation exceeding 3200 mm annually, the most extreme values across all precipitation indices,

and relatively short dry periods. Finally, the Transitional Zone accounts for 19% of the area and displays intermediate characteristics between the other regimes, with high spatial variability reflecting the complex topographic influences and competing moisture sources in these areas.

**Table 3.** Spatial Clustering Results Summary

| Cluster | Area (%) | Mean PRCPTOT (mm) | Mean CDD (days) | Mean SDII (mm/day) | Dominant Process |
|---|---|---|---|---|---|
| Northern Coastal | 22 | 1,847 ± 156 | 52.3 ± 8.2 | 12.4 ± 1.1 | Rain shadow effect |
| Central Highland | 31 | 3,124 ± 298 | 28.7 ± 5.4 | 16.8 ± 1.8 | Orographic lifting |
| Southern Mountain | 28 | 3,421 ± 187 | 21.2 ± 4.1 | 17.9 ± 2.1 | Convergence zones |
| Transitional | 19 | 2,563 ± 445 | 38.9 ± 12.7 | 14.7 ± 2.8 | Mixed processes |

Maximum consecutive dry days (CDD) display inverse patterns with longest dry periods (44-64 days) occurring in northern coastal areas, reflecting rain shadow effects and differential monsoon moisture penetration. This spatial pattern has important implications for agricultural planning and water resource management.

## Physical Mechanisms and Climate Implications

### Ocean-Atmosphere Feedback Mechanisms

The identified lag relationships between precipitation and chlorophyll-a provide insights into underlying physical mechanisms operating in the West Java coastal system. The 19-day lead time suggests that terrestrial precipitation events serve as a precursor to marine ecosystem changes through modification of coastal water properties and nutrient cycling.

When precipitation events exceed threshold values (~10 mm/day), enhanced freshwater runoff increases surface stratification and reduces vertical mixing efficiency. This mechanism operates through density gradients created by freshwater input, which inhibit nutrient transport from deeper waters to the euphotic zone where phytoplankton growth occurs.

Surface salinity calculations indicate that heavy precipitation events (>20 mm/day) can reduce coastal salinity by 2-4 psu within 1-2 weeks, sufficient to create stable density stratification and suppress primary productivity. The delayed ecosystem response reflects the time required for runoff transport, mixing processes, and biological community adjustment.

### Climate Change Implications

Climate change projections suggest continued intensification of extreme precipitation events under warming scenarios [34], [35]. The relationships identified in this study indicate that such changes may affect marine ecosystem productivity through enhanced stratification and altered nutrient cycling processes.

Based on the observed sensitivities, increased precipitation intensity could potentially increase the frequency of marine productivity suppression events. However, these relationships require validation through coupled climate-ecosystem modeling to account for non-linear feedbacks, threshold effects, and interactions with other environmental factors including temperature, ocean circulation, and large-scale climate variability

### Predictive Applications and Early Warning Systems

#### Forecast Skill Assessment

The significant correlation between precipitation and chlorophyll-a with 19-day lead time provides valuable information for ecosystem monitoring and management. Cross-wavelet coherence analysis demonstrates consistent phase relationships across multiple temporal scales, supporting the development of operational prediction systems.

A simple linear regression model using SST anomalies explains 3% of chlorophyll-a variance at 19-day lead time:

$$\text{Chl-a}(t+19) = -0.173 \times \text{Precipitation\_anomaly}(t) + \varepsilon \quad (7)$$

While modest, this relationship provides statistically significant predictive capability for marine ecosystem monitoring, particularly when combined with spectral analysis techniques that capture periodic variations.

#### Operational Implementation

The relationships identified offer potential integration into operational marine ecosystem monitoring systems. Real-time precipitation monitoring using satellite observations with daily latency enables rapid detection of runoff events relevant to coastal productivity changes. Threshold-based alerting protocols can flag persistent precipitation anomalies exceeding +2 standard deviations for durations longer than one week.

Multi-variate indices combining precipitation patterns, seasonal cycles, and large-scale climate modes provide a more comprehensive basis for anticipating ecosystem responses. These forecast products can inform marine protected area management, fisheries planning, and coastal water quality monitoring programs.

## 4 Conclusion

This study provides compelling evidence for significant ocean-atmosphere-ecosystem coupling in West Java, with statistically robust relationships identified through multiple analytical approaches. The integration of cross-wavelet coherence analysis with traditional correlation methods strengthens the evidence for systematic phase relationships, while spatial clustering analysis reveals the geographic heterogeneity of extreme precipitation patterns.

The 19-day lead time between precipitation and chlorophyll-a changes, validated through both time-domain correlation ($r = -0.173$, $p < 0.001$) and spectral-domain coherence analysis (78% annual coherence), provides clear evidence of terrestrial runoff impacts on marine ecosystem productivity. The cross-wavelet analysis reveals that this coupling mechanism operates consistently across multiple temporal scales, from intraseasonal (30-90 days) to interannual (2-4 years) variability.

The identification of four distinct precipitation regimes through k-means clustering, validated by significant spatial autocorrelation (Moran's I = 0.65-0.89) and strong cluster structure (silhouette score = 0.67), demonstrates the importance of considering local geographic controls in climate extremes analysis. This spatial heterogeneity has important implications for region-specific adaptation strategies and water resource management planning.

Beyond advancing scientific understanding of tropical ocean-atmosphere-ecosystem interactions, these findings provide a foundation for operational applications. The systematic lag relationships offer predictive potential for marine ecosystem monitoring, while the spectral coherence analysis provides confidence

intervals for forecast skill assessment. The comprehensive spatial analysis framework can be adapted to other coastal regions facing similar climate vulnerabilities.

Future research should incorporate broader climate drivers including ENSO and IOD indices, along with high-resolution coupled ocean-atmosphere modeling to enhance prediction capabilities and support climate adaptation planning across the Indonesian maritime continent. The methodological integration of satellite observations with advanced time-series analysis demonstrated here provides a robust framework for understanding complex Earth system interactions in tropical regions.

## 6. Acknowledgements

The authors acknowledge NASA Goddard Space Flight Center for providing IMERG precipitation and MODIS Ocean Color data through the Giovanni online data system. We thank the Indonesian Agency for Meteorology, Climatology and Geophysics (BMKG) for providing validation data and the University of Padjadjaran for institutional support.

## 7. Referensi

[1] E. Aldrian and R. D. Susanto, "Identification of three dominant rainfall regions within Indonesia and their relationship to sea surface temperature," *International Journal of Climatology*, vol. 23, no. 12, pp. 1435–1452, Oct. 2003.

[2] J.-H. Qian, A. W. Robertson, and V. Moron, "Diurnal Cycle in Different Weather Regimes and Rainfall Variability over Borneo Associated with ENSO," *J. Clim.*, vol. 26, no. 5, pp. 1772–1790, Mar. 2013.

[3] Supari, F. Tangang, L. Juneng, and E. Aldrian, "Observed changes in extreme temperature and precipitation over Indonesia," *International Journal of Climatology*, vol. 37, no. 4, pp. 1979–1997, 2017.

[4] F. Tangang *et al.*, "Projected future changes in rainfall in Southeast Asia based on CORDEX–SEA multi-model simulations," *Clim. Dyn.*, vol. 55, no. 5–6, pp. 1247–1267, Sep. 2020.

[5] M. Komunikasi dan Pengembangan Teknik Lingkungan, J. Panggabean, F. Syamsudin, N. Purba, and X. Feng, "Jurnal Presipitasi Interannual Climate Variability Impacts on Rainfall Extremes and Flooding," *Jurnal Presipitasi Media Komunikasi dan Pengembangan Teknik Lingkungan*, vol. 23, no. 1, pp. 244–257, 2026.

[6] M. A. Marfai and L. King, "Potential vulnerability implications of coastal inundation due to sea level rise for the coastal zone of Semarang city, Indonesia," *Environmental Geology*, vol. 54, no. 6, pp. 1235–1245, May 2008.

[7] M. K. Roxy *et al.*, "Indian Ocean Warming," in *Assessment of Climate Change over the Indian Region*, Singapore: Springer Singapore, 2020, ch. 10, pp. 191–206.

[8] C. Zhang, F. Adames, B. Khouider, B. Wang, and D. Yang, "Four Theories of the Madden-Julian Oscillation," *Reviews of Geophysics*, vol. 58, no. 3, 2020.

[9] T. Horii, I. Ueki, E. Siswanto, and I. Iskandar, "Long-term shift and recent early onset of chlorophyll-a bloom and coastal upwelling along the southern coast of Java," *Frontiers in Climate*, vol. 5, Apr. 2023, doi: 10.3389/fclim.2023.1050790.

[10] X. Liu, M. Wang, and W. Shi, "A study of a Hurricane Katrina-induced phytoplankton bloom using satellite observations and model simulations," *J. Geophys. Res. Oceans*, vol. 114, no. 3, pp. 1–12, Mar. 2009.

[11] E. Siswanto *et al.*, "Empirical ocean-color algorithms to retrieve chlorophyll-a, total suspended matter, and colored dissolved organic matter absorption coefficient in the Yellow and East China Seas," *J. Oceanogr.*, vol. 67, no. 5, pp. 627–650, Oct. 2011, doi: 10.1007/s10872-011-0062-z.

[12] J. Tan, W. A. Petersen, and A. Tokay, "A Novel Approach to Identify Sources of Errors in IMERG for GPM Ground Validation," *J. Hydrometeorol.*, vol. 17, no. 9, pp. 2477–2491, Sep. 2016.
[13] G. Huffman *et al.*, "NASA GPM Integrated Multi-satellitE Retrievals for GPM (IMERG) Algorithm Theoretical Basis Document (ATBD) Version 06," *Nasa/Gsfc*, p. p30, 2020.
[14] J. Panggabean *et al.*, "Satellite-Based Atmospheric Monitoring for Environmentally Resilient Smart Cities in Indonesia", doi: 10.24815/jr.v8i4.49740.
[15] J. W. Campbell *et al.*, "Comparison of algorithms for estimating ocean primary production from surface chlorophyll, temperature, and irradiance," *Global Biogeochem. Cycles*, vol. 16, no. 3, pp. 9-1-9–15, Sep. 2002.
[16] C. Hu, Z. Lee, and B. Franz, "Chlorophyll a algorithms for oligotrophic oceans: A novel approach based on three-band reflectance difference," *J. Geophys. Res. Oceans*, vol. 117, no. 1, pp. 1–25, Jan. 2012.
[17] W. Cai *et al.*, "Increasing frequency of extreme El Niño events due to greenhouse warming," *Nat. Clim. Chang.*, vol. 4, no. 2, pp. 111–116, 2014.
[18] H. H. Hendon, "Indonesian rainfall variability: Impacts of ENSO and local air-sea interaction," *J. Clim.*, vol. 16, no. 11, pp. 1775–1790, Jun. 2003.
[19] N. H. Saji, B. N. Goswami, P. N. Vinayachandran, and T. Yamagata, "A dipole mode in the tropical Indian Ocean," *Nature*, vol. 401, no. 6751, pp. 360–363, Sep. 1999.
[20] J. Panggabean, H. Fawwaz Putra, and K. Khosyi Counedio, "CLIMATE-SECURITY NEXUS: ENSO-DRIVEN RAINFALL VARIABILITY AND MARITIME SECURITY VULNERABILITY IN INDONESIAN STRATEGIC WATERS," *Pusat Pengkajian Maritim Seskoal Indonesia*, vol. 5, no. 2, pp. 39–62, 2025.
[21] A. L. Gordon, B. A. Huber, E. J. Metzger, R. D. Susanto, H. E. Hurlburt, and T. R. Adi, "South China Sea throughflow impact on the Indonesian throughflow," *Geophys. Res. Lett.*, vol. 39, no. 11, pp. 1–7, Jun. 2012.
[22] E. Siswanto, J. Ishizaka, S. C. Tripathy, and K. Miyamura, "Detection of harmful algal blooms of Karenia mikimotoi using MODIS measurements: A case study of Seto-Inland Sea, Japan," *Remote Sens. Environ.*, vol. 129, pp. 185–196, Feb. 2013.
[23] M. J. Behrenfeld *et al.*, "Climate-driven trends in contemporary ocean productivity," *Nature*, vol. 444, no. 7120, pp. 752–755, Dec. 2006.
[24] NASA, "MODIS Ocean Color Data Processing Guidelines," NASA Ocean Color Web.
[25] P. Jönsson and L. Eklundh, "TIMESAT—a program for analyzing time-series of satellite sensor data," *Comput. Geosci.*, vol. 30, no. 8, pp. 833–845, Oct. 2004, doi: 10.1016/j.cageo.2004.05.006.
[26] A. M. G. Klein Tank, F. W. Zwiers, and X. Zhang, *Guidelines on analysis of extremes in a changing climate in support of informed decisions for adaptation*. WMO, 2009.
[27] X. Zhang *et al.*, "Indices for monitoring changes in extremes based on daily temperature and precipitation data," *WIREs Climate Change*, vol. 2, no. 6, pp. 851–870, Nov. 2011, doi: 10.1002/wcc.147.
[28] Y. Hu, *Water Tower of the Yellow River in a Changing Climate: Toward an integrated assessment*. CRC Press/Balkema, 2014.
[29] C. Torrence and G. P. Compo, "A Practical Guide to Wavelet Analysis," *Bull. Am. Meteorol. Soc.*, vol. 79, no. 1, pp. 61–78, Jan. 1998.
[30] A. Grinsted, J. C. Moore, and S. Jevrejeva, "Application of the cross wavelet transform and wavelet coherence to geophysical time series," *Nonlinear Process. Geophys.*, vol. 11, no. 5/6, pp. 561–566, Nov. 2004, doi: 10.5194/npg-11-561-2004.
[31] B. Podobnik and H. E. Stanley, "Detrended Cross-Correlation Analysis: A New Method for Analyzing Two Non-stationary Time Series," *Phys. Rev. Lett.*, vol. 100, no. 8, p. 084102, Sep. 2007.

[32] C. S. Bretherton, M. Widmann, V. P. Dymnikov, J. M. Wallace, and I. Bladé, "The effective number of spatial degrees of freedom of a time-varying field," *J. Clim.*, vol. 12, no. 7, pp. 1990–2009, Jul. 1999.

[33] D. F. Sinaga[1], F. Humaira[1], K. T. J. Sinurat[1], F. A. R. Priatnam[1], and J. Panggabean[1], "Topographic Enhancement of Extreme Rainfall in IKN Nusantara Based on Multi-Satellite Observations," *Jurnal Penelitian Fisika dan Terapannya (Jupiter)*, vol. 7, no. 2, pp. 1–11, 2026, doi: 10.31851/jupiter.v7i2.

[34] IPCC, *Climate Change 2021 – The Physical Science Basis. Contribution of Working Group I to the Sixth Assessment Report of the Intergovernmental Panel on Climate Change*. Geneva: Cambridge University Press, 2021.

[35] J. Panggabean, J. Kurnia, and T. Shaumul, "Sea Level Rise Impacts on Coastal Oil Palm Plantations," *International Journal of Oil Palm*, vol. 8, no. 1, pp. 1–14, 2025, doi: 10.35876/ijop.v8i1.138.